

AD-A099 978

NATIONAL BUREAU OF STANDARDS WASHINGTON DC SURFACE S--ETC F/G 7/3  
SEARCH FOR CHEMISORBED HCO: THE INTERACTION OF FORMALDEHYDE, GL--ETC(U)  
MAY 81 Y T YATES, R R CAVANAGH N00014-81-F-0008

UNCLASSIFIED

TR-22

NL

1 of 1  
AD-A  
1009978


END  
DATE  
FILMED  
6-81  
DTIC

AD A099970

① LEVEL II

OFFICE OF NAVAL RESEARCH  
Contract 14-81-F-0008

SC

Technical Report #22

Search for Chemisorbed HCO: The Interaction of  
Formaldehyde, Glyoxal and Atomic Hydrogen + CO with Rh

J. T. Yates, Jr. and R. R. Cavanagh

Surface Science Division  
National Bureau of Standards  
Washington, DC 20234

DTIC  
ELECTE  
JUN 10 1981  
S B D

May, 1981

Reproduction in whole or in part is permitted for any purpose  
of the United States Government

Approved for Public Release; Distribution Unlimited

To be published in Journal of Catalysis

DTIC FILE COPY

81 6 05 027

REPORT DOCUMENTATION PAGE		READ INSTRUCTIONS BEFORE COMPLETING FORM
1. REPORT NUMBER	2. GOVT ACCESSION NO.	3. RECIPIENT'S CATALOG NUMBER
⑨ Technical Report No. 22	AD-A099 970	
4. TITLE (and Subtitle)	5. TYPE OF REPORT & PERIOD COVERED	
⑥ Search for Chemisorbed HCO: The Interaction of Formaldehyde, Glyoxal and Atomic Hydrogen + CO with Rh.	⑭ TR-22	
7. AUTHOR(s)	6. PERFORMING ORG. REPORT NUMBER	
⑩ J. T. Yates, Jr. R. R. Cavanagh	⑦ CONTRACT OR GRANT NUMBER(s)	
	⑮ 14-81-F-0008 New Mod. No. P00001	
9. PERFORMING ORGANIZATION NAME AND ADDRESS	10. PROGRAM ELEMENT, PROJECT, TASK AREA & WORK UNIT NUMBERS	
Surface Science Division National Bureau of Standards Washington, DC 20234	⑫ 34	
11. CONTROLLING OFFICE NAME AND ADDRESS	12. REPORT DATE	13. NUMBER OF PAGES
	⑪ May 81	
14. MONITORING AGENCY NAME & ADDRESS (if different from Controlling Office)	15. SECURITY CLASS. (of this report)	
	Unclassified	
16. DISTRIBUTION STATEMENT (of this Report)		
Approved for Public Release; Distribution Unlimited		
17. DISTRIBUTION STATEMENT (of the abstract entered in Block 20, if different from Report)		
18. SUPPLEMENTARY NOTES		
Preprint; to be published in Journal of Catalysis		
19. KEY WORDS (Continue on reverse side if necessary and identify by block number)		
Chemisorption; formaldehyde; formyl; glyoxal; Rh.		
20. ABSTRACT (Continue on reverse side if necessary and identify by block number)		
<p>Transmission infrared spectroscopy has been used to search for the chemisorptive-stabilization of formyl (HCO) on Al<sub>2</sub>O<sub>3</sub>-supported Rh surfaces. Formaldehyde (H<sub>2</sub>CO) and glyoxal (HCO)<sub>2</sub> have been used as potential sources of HCO. In addition, chemisorbed CO on Rh has been treated with atomic deuterium in an attempt to produce DCO. None of these routes have led to spectroscopically detectable levels of formyl adsorption at temperatures near or above 100K. These results suggest that the formyl intermediate may not be a stable surface species on Rh in CO-hydrogenation chemistry.</p>		

P 12

SEARCH FOR CHEMISORBED HCO: THE INTERACTION OF FORMALDEHYDE,  
GLYOXAL AND ATOMIC HYDROGEN + CO WITH Rh

J. T. Yates, Jr.

and

R. R. Cavanagh\*\*

Surface Science Division

National Bureau of Standards

Washington, D.C. 20234

\*NRC-NBS Postdoctoral Research Associate 1979-1981 +Present address:  
Molecular Spectroscopy Division, National Bureau of Standards,  
Washington, DC 20234

SEARCH FOR CHEMISORBED HCO: THE INTERACTION OF FORMALDEHYDE,  
GLYOXAL AND ATOMIC HYDROGEN + CO WITH Rh

J. T. Yates, Jr.

and

R. R. Cavanagh

Surface Science Division

National Bureau of Standards

Washington, D.C. 20234

ABSTRACT

Transmission infrared spectroscopy has been used to search for the chemisorptive-stabilization of formyl (HCO) on  $\text{Al}_2\text{O}_3$ -supported Rh surfaces. Formaldehyde ( $\text{H}_2\text{CO}$ ) and glyoxal ( $\text{HCO})_2$  have been used as potential sources of HCO. In addition, chemisorbed CO on Rh has been treated with atomic deuterium in an attempt to produce DCO. None of these routes have led to spectroscopically detectable levels of formyl adsorption at temperatures near or above 100K. These results suggest that the formyl intermediate may not be a stable surface species on Rh in CO-hydrogenation chemistry.

Accession For	
NTIS GRA&I	<input checked="checked" type="checkbox"/>
DTIC TAB	<input type="checkbox"/>
Unannounced	<input type="checkbox"/>
Justification	
By	
Distribution/	
Availability Codes	
Dist	Avail and/or Special
A	

SEARCH FOR CHEMISORBED HCO: THE INTERACTION  
OF FORMALDEHYDE, GLYOXAL AND ATOMIC HYDROGEN + CO WITH Rh

J. T. Yates, Jr. and R. R. Cavanagh

Surface Science Division

National Bureau of Standards

Washington, D.C. 20234

I. INTRODUCTION

Mechanistic details of the catalytic production of  $\text{CH}_4$  and larger hydrocarbons from  $\text{H}_2(\text{g}) + \text{CO}(\text{g})$  have been the subject of much recent speculation. Experimental studies in coupled high pressure/ultra high vacuum systems have demonstrated the active role of surface carbon (or  $\text{CH}_x$  species) on Ni single crystals in such reactions. (1) The capacity to form  $\text{CH}_4$  from the reaction with  $\text{H}_2(\text{g})$  of CO-produced surface carbon indicates that CO dissociation is a compatible first step in the catalytic reaction pathway to  $\text{CH}_4$ . Further studies of various types have supported the CO dissociation mechanism on Ru (2-4). Similar conclusions have been reached regarding C formation from CO on polycrystalline Rh surfaces (5), and in particular on stepped Rh single crystals (6,7), although the efficiency of CO dissociation processes on Rh is a controversial issue at present (7).

Contrary to a model involving dissociative CO chemisorption as the primary elementary step in the catalytic formation of hydrocarbons, mechanisms involving the hydrogenation of CO to form various intermediates such as  $\text{HCO}(\text{ads})$  or  $\text{HCOH}(\text{ads})$  have also been widely discussed in the recent literature, as exemplified in a review article by Muettertides and

Stein (8), as well as in earlier reviews (9). In addition, experimental observations which detected small quantities of  $\text{CH}_4$  produced from  $\text{H}_2\text{CO}$  chemisorption on  $\text{Ru}(110)$  (10) and on  $\text{W}(100)$  and  $\text{W}(111)$  (11, 12) have lent support to the alternate model, in which species like adsorbed formyl,  $\text{HCO}(\text{ads})$ , are postulated to be involved in the catalytic synthesis of  $\text{CH}_4$  from  $\text{CO}$  and  $\text{H}_2$ . While the exact role played by these species during a chemical reaction is not known, the synthesis of model inorganic compounds containing such functional groups clearly demonstrates their existence (13).

The work to be discussed in this paper addresses the question of the stabilization of species like  $\text{HCO}(\text{ads})$  on an  $\text{Al}_2\text{O}_3$ -supported Rh surface. We have employed molecules such as  $\text{H}_2\text{CO}$  and  $(\text{HCO})_2$  as adsorbates at 100 K. Transmission infrared spectroscopy was used to search for intermediates in the catalytic decomposition of these molecules as the surface was warmed to 340 K. In addition, atomic deuterium was employed as a reactant with chemisorbed  $\text{CO}$  on Rh in an attempt to produce  $\text{DCO}(\text{ads})$ .

The combination of low temperature adsorption techniques with infrared spectroscopy on supported metal systems is a potentially promising method for trapping and observing such transient reaction intermediates. Temperature dependent surface binding state distributions between 77 and 300K are well known on single crystal substrates from investigations using a variety of surface sensitive spectroscopies, yet rarely have such species been studied using the infrared transmission technique. The combination of low temperature methods with model adsorbate systems provides a unique opportunity to prepare, isolate, and study various proposed reaction intermediates.

## II. EXPERIMENTAL

Complete details of the sample preparation, vacuum system, and spectrometer have appeared elsewhere (14, 15). In brief, a solution of  $\text{Rh}^{\text{III}}$  ions was prepared by dissolving  $\text{RhCl}_3 \cdot 3\text{H}_2\text{O}$  in water. This mixture was then used to impregnate an amount of  $\text{Al}_2\text{O}_3$  (DeGussa-C)\*\* such that the weight percentage of rhodium would be 2.2%. Acetone was then added to the solution (10:1 = acetone:water). This slurry was sprayed onto a  $\text{CaF}_2$  plate held at 350K causing flash evaporation of solvents. Typical deposit loadings of  $11\text{mg}/\text{cm}^2$  were obtained. The deposited sample was then mounted in the ultrahigh vacuum infrared cell, outgassed at 425K, reduced in  $\text{H}_2$  at 425K, and further outgassed at 475K for eight hours. All infrared spectra were recorded on a Perkin Elmer Model 180 Infrared Spectrometer\*\*.

$\text{H}_2\text{CO}(\text{g})$  was prepared by heating paraformaldehyde in a gas generator at 350K, passing the gas through a glass trap at 195K, and directly admitting the  $\text{H}_2\text{CO}(\text{g})$  to the stainless steel manifold. The purity of the  $\text{H}_2\text{CO}(\text{g})$  obtained by this method is well established (11).

$(\text{CHO})_2(\text{g})$  was obtained using established literature methods (16). A mixture of  $\text{P}_2\text{O}_5$  and trimeric glyoxal dihydrate  $(\text{C}_2\text{H}_2\text{O}_2)_3 \cdot (2\text{H}_2\text{O})$  (1:1) was placed in a glass system similar to that used for the formaldehyde generator. The generator was evacuated and the glass trap immersed in liquid nitrogen. While pumping on the generator/trap, the mixture was gently heated. In addition to the evolution of non-condensable gases, both yellow crystals and white crystals appeared in the glass trap. The  $\text{P}_2\text{O}_5/(\text{C}_2\text{H}_2\text{O}_2)_3 \cdot (2\text{H}_2\text{O})$  vessel was isolated from the trap, and the trap was brought to 195K, at which time the evolution of additional non-

condensibles and the disappearance of the white crystals was noted. The remaining yellow crystals were further purified by a freeze-pump-thaw cycle. The pressure of an aliquot of vapor obtained upon warming from this purified sample was found to be stable in the stainless steel manifold to 0.1% over several minutes.

The generation of deuterium atoms was achieved with a thermal source operating in a  $D_2$  atmosphere. In these experiments, a high temperature tungsten filament was operated inside the infrared cell (see Figure 1). The adsorbent was shielded from radiation from the filament by means of a baffle arrangement. The  $D_2$  gas phase pressure in the range 0.2 torr-0.01 torr was monitored with a capacitance manometer as a function of filament temperature; we observed the initiation of a continuous pressure drop at the onset of D atom generation. This is presumably due to interaction of D atoms with the cell walls or the sample.

Due to the location of the thermocouple on the copper sample holder rather than within the sample itself, there is some uncertainty as to the exact temperature of the specimen. Rather than attempt to correct for this error, the temperatures given refer simply to the temperature of the copper support assembly.

### III. INTERACTION OF FORMALDEHYDE WITH $Al_2O_3$ AND WITH $Rh/Al_2O_3$ .

#### A. $H_2CO$ Adsorbed on $Al_2O_3$

A Rh free sample of  $Al_2O_3$  weighing 58mg was prepared as described in the experimental section. This sample was then cooled to  $\sim 100K$  and exposed to  $6 \times 10^{19}$  molecules of  $H_2CO(g)$ . This dose of  $H_2CO$  corresponded

to  $\sim 1$  molecule per  $10\text{\AA}^2$  of  $\text{Al}_2\text{O}_3$  surface area. Following measurement of the infrared spectrum, the surface was warmed in a stepwise fashion to 300K and spectral developments were followed, as shown in Fig. 2. Finally, at 300K, the cell was evacuated and spectrum 2e was recorded.

At 160K, a distinct feature due to physisorbed  $\text{H}_2\text{CO}$  develops near  $1700\text{cm}^{-1}$ ; upon warming the dosed cell to 300K, the  $1700\text{cm}^{-1}$  feature has diminished in intensity, while additional absorbance due to  $\text{H}_2\text{CO(g)}$  develops near  $1750\text{cm}^{-1}$ . After evacuation at 300K, there is little evidence for either feature. However, new features which appear at  $1591\text{cm}^{-1}$ ,  $1392\text{cm}^{-1}$  and  $1372\text{cm}^{-1}$  persist upon evacuation. These three features are in excellent agreement with those reported for formate production from  $\text{CH}_3\text{OH}$  decomposition on  $\text{Al}_2\text{O}_3$  [ $1597\text{cm}^{-1}$ ;  $1394\text{cm}^{-1}$ ;  $1377\text{cm}^{-1}$ ] (17).

The region between  $2700\text{cm}^{-1}$  and  $2000\text{cm}^{-1}$  was carefully examined during this experiment, since this is the region in which the H-C stretching frequency for  $\text{HCO(ads)}$  would be expected. The only additional feature which appeared was a broad weak feature near  $2040\text{cm}^{-1}$  (6% of the  $1700\text{cm}^{-1}$  peak intensity). This feature disappears upon evacuation at 300K. Table I summarizes the observed spectral features in this series of measurements.

#### B. $\text{H}_2\text{CO}$ Adsorbed on $\text{Rh/Al}_2\text{O}_3$

A 61 mg sample containing 2.2% Rh was prepared. Following cooling to 100K, the sample was exposed to  $8 \times 10^{18}$  molecules of  $\text{H}_2\text{CO(g)}$ . From previous experiments we know that the chemisorptive capacity of this  $\text{Rh/Al}_2\text{O}_3$  sample for  $\text{CO(g)}$  should be  $\sim 1.1 \times 10^{19}$  CO molecules (18).

The spectral development as a function of temperature is shown in Fig. 3. The spectral feature observed near  $1700\text{cm}^{-1}$  at 160K can be associated with  $\text{H}_2\text{CO}$  physisorbed on  $\text{Al}_2\text{O}_3$ , as seen for pure  $\text{Al}_2\text{O}_3$  in Fig. 2. As the  $\text{Rh}/\text{Al}_2\text{O}_3$  sample is warmed, the development of additional spectral features between  $2100$  and  $1800\text{cm}^{-1}$  is apparent. At 230K spectral features at  $1860$ ,  $2021$ ,  $2045$  and  $2088\text{cm}^{-1}$  are observed as well as H-C stretching modes at  $\sim 2910$  and  $\sim 2980\text{cm}^{-1}$ . An additional weak feature at  $\sim 2790\text{cm}^{-1}$  is also observed.

Previous work has shown that the  $1860\text{cm}^{-1}$  feature can be assigned to bridge-bonded CO (14, 19, 20) on Rh crystallite sites. For pure CO adsorption, features in the  $2000$ - $2100\text{cm}^{-1}$  region have been assigned to terminal CO species on Rh crystallites [ $\sim 2050$ - $2070\text{cm}^{-1}$ ] (14) and to  $\text{Rh}(\text{CO})_2$  species produced on isolated Rh sites [ $2101$ ;  $2031\text{cm}^{-1}$ ] (14,18). The features at  $2088\text{cm}^{-1}$  and  $2021\text{cm}^{-1}$ , as produced by  $\text{H}_2\text{CO}(\text{g})$  adsorption, are  $\sim 10\text{cm}^{-1}$  lower in wavenumber than the corresponding features produced by  $\text{CO}(\text{g})$  adsorption, in agreement with earlier observations for  $\text{H}_2\text{CO}$  adsorption on  $\text{Rh}/\text{Al}_2\text{O}_3$  (21). This  $10\text{cm}^{-1}$  shift will be discussed in section III.C.

It should be noted here that the intensity of absorbance in the  $2100$  to  $1800\text{cm}^{-1}$  region for all of these features derived from  $\text{H}_2\text{CO}(\text{g})$  adsorption is much lower than expected for full CO coverage. This observation is confirmed also from the experiment shown in spectrum 3d where the  $\text{H}_2\text{CO}(\text{g})$  was pumped from the cell and  $^{12}\text{CO}(\text{g})$  was introduced. The significant increase in absorbance at  $1860$ ,  $2020$ ,  $2050$ , and  $2093\text{cm}^{-1}$  indicates the presence of active Rh sites for CO chemisorption in spite of the high dose of  $\text{H}_2\text{CO}(\text{g})$ .

C. Perturbation of Rh-Chemisorbed CO Species by Adsorbates  
on the  $\text{Al}_2\text{O}_3$  Support.

It is possible that small spectral shifts for chemisorbed CO on  $\text{Al}_2\text{O}_3$ -supported Rh could be due to interactions with adsorbed CO caused by adsorption of other molecules on the  $\text{Al}_2\text{O}_3$  support, in much the same fashion as observed in matrix isolation infrared spectroscopy for changes in the matrix. Two experiments were carried out in order to check this point:

1.  $\text{H}_2\text{O} + \text{CO/Rh/Al}_2\text{O}_3$ .

A Rh/ $\text{Al}_2\text{O}_3$  sample was exposed to  $\text{H}_2\text{O}(\text{g})$  at 0.5 torr pressure. Increased absorbance was observed in the OH stretching region between 3700 and  $3000\text{cm}^{-1}$  and a feature due to  $\text{H}_2\text{O}$  adsorption on  $\text{Al}_2\text{O}_3$  is observed in the HOH bending region near  $1620\text{cm}^{-1}$ . Only minor changes in CO-derived spectral features on Rh were observed when the evacuated sample was subsequently exposed to  $\text{CO}(\text{g})$ ; spectral features at 2098, 2053, 2027 and  $1860\text{cm}^{-1}$  were produced. This corresponds to an approximately  $2\text{-}3\text{cm}^{-1}$  decrease in wavenumber for the doublet from values of 2101 and  $2031\text{cm}^{-1}$  observed on  $\text{H}_2\text{O}$  free surfaces.

2.  $\text{H}_2^{13}\text{CO} + \text{CO/Rh/Al}_2\text{O}_3$ .

In a separate experiment, a 2.2% Rh sample was saturated with  $^{13}\text{CO}$  and evacuated (see Fig. 4) resulting in  $^{13}\text{CO}$  features at 2053, 2035,

1987, and  $1825\text{cm}^{-1}$ . This sample was subsequently exposed to a saturation coverage of  $\text{H}_2^{12}\text{CO}$  [see Fig. 4(c)]. The features previously associated with the formation of formates on the  $\text{Al}_2\text{O}_3$  are clearly present. In addition, the two sharp IR peaks associated with  $^{13}\text{CO}$  bound to Rh as  $\text{Rh}(\text{CO})_2$  were observed to shift to lower wavenumber by  $10\text{cm}^{-1}$  to  $2042$  and  $1975\text{cm}^{-1}$ . Introduction of additional  $\text{H}_2\text{CO}$  resulted in a further shift of the  $^{13}\text{CO}$  features. The significant shift in the  $^{13}\text{CO}$  features, and the absence of infrared evidence for  $^{12}\text{CO}$ - $^{13}\text{CO}$  exchange demonstrates a strong support perturbation of the Rh-bound CO modes attributable to the presence of oxide-bound species derived from  $\text{H}_2\text{CO}$ .

#### IV. Interaction of Glyoxal with $\text{Al}_2\text{O}_3$ and with Rh/ $\text{Al}_2\text{O}_3$ .

##### A. $(\text{HCO})_2$ Adsorbed on $\text{Al}_2\text{O}_3$ .

In Fig. 5, a 55mg sample of  $\text{Al}_2\text{O}_3$  was exposed to  $4 \times 10^{19}$   $(\text{HCO})_2(\text{g})$  molecules at 100K and then warmed. Infrared spectra as a function of sample temperature are shown. Spectrum 5(a) indicates the presence of very little adsorbate on the  $\text{Al}_2\text{O}_3$ , presumably because of condensation of the  $(\text{HCO})_2(\text{g})$  on cooler regions of the sample support assembly. Upon warming to 190K, two predominant peaks at  $1720\text{cm}^{-1}$  and  $1748\text{cm}^{-1}$  are observed as  $(\text{HCO})_2$  transfers to the  $\text{Al}_2\text{O}_3$ . Between 235K and 275K, an inversion of relative intensity occurs as the intensity of the  $1720\text{cm}^{-1}$  feature decreases while the intensity of the  $1748\text{cm}^{-1}$  feature increases. The only other features observed between  $3200\text{cm}^{-1}$  and  $1400\text{cm}^{-1}$  were bands at  $2930\text{cm}^{-1}$  and  $2840\text{cm}^{-1}$ . There are small changes in the relative

intensity of these two bands during sample warming, but both bands persist upon evacuation of the cell. The behavior observed on warming the  $\text{Al}_2\text{O}_3$  surface from 190K to 305K is not observed to be reversible upon subsequent cooling back to 100K. The presence of an intense feature at  $1748\text{cm}^{-1}$  upon evacuation at 305K is in distinct contrast to the behavior observed for  $\text{H}_2\text{CO}$  on  $\text{Al}_2\text{O}_3$  (Fig. 2), where irreversibly adsorbed formate species are produced.

B.  $(\text{HCO})_2$  Adsorbed on Rh/ $\text{Al}_2\text{O}_3$

The adsorption of  $(\text{HCO})_2(\text{g})$  on a 2.3% Rh sample weighing 90mg is shown in Fig. 6. By comparison with data obtained for pure  $\text{Al}_2\text{O}_3$  (Fig. 5) it may be seen that the behavior in the  $1700\text{-}1800\text{cm}^{-1}$  region and in the  $2800\text{-}3000\text{cm}^{-1}$  region is very similar, suggesting that these spectral features are unrelated to the interaction of  $(\text{HCO})_2$  with Rh. At temperatures above 190K, new infrared features in the  $1800\text{-}2100\text{cm}^{-1}$  region are observed due to the interaction of  $(\text{HCO})_2$  with Rh. Comparing glyoxal spectrum 5(c) with formaldehyde spectrum 3(c) suggests that the infrared spectrum of the species-present on the Rh sites are very similar although relative intensities differ somewhat. Thus in each case we observe major bands at  $\sim 2045$  and  $\sim 1860\text{cm}^{-1}$  similar to those observed for low coverages of  $\text{CO}(\text{ads})$  on crystalline Rh sites (14,18). In addition small features at  $\sim 2090\text{cm}^{-1}$  and  $\sim 2020\text{cm}^{-1}$  are observed in both cases, indicative of formation of relatively small amounts of  $\text{Rh}(\text{CO})_2$  (14,18). It is observed that the intensities of all of these features due to  $(\text{HCO})_2$  adsorption is below that observed for  $\text{CO}(\text{g})$  adsorption.

Subsequent CO exposure of the  $(\text{HCO})_2$ -exposed Rh/ $\text{Al}_2\text{O}_3$  sample at 300K causes full development of the expected features due to CO(ads) as shown in Fig. 6(e). Thus, exposure to a large dose of  $(\text{HCO})_2(\text{g})$  does not cause full occupancy of all Rh sites capable of CO adsorption. Similar behavior was also observed with the  $\text{H}_2\text{CO}$  adsorbate.

#### V. INTERACTION OF MOLECULAR AND ATOMIC HYDROGEN WITH CO ADSORBED ON Rh.

In earlier work, the exposure of dispersed Rh on  $\text{Al}_2\text{O}_3$  to a mixture of  $\text{H}_2(\text{g})$  and  $\text{CO}(\text{g})$  at 300K resulted in comparable infrared spectra to that obtained for pure CO exposures (21). In addition, LEED studies and thermal desorption studies have indicated that repulsive CO(ads)-H(ads) interactions occur on Rh(111), leading to a lowering of the desorption energy for H(ads) (22). Thus it might be expected that the competition between  $\text{H}_2(\text{g})$  and  $\text{CO}(\text{g})$  for Rh adsorption sites would favor CO if the temperature is sufficiently high, permitting rapid  $\text{H}_2$  desorption following addition of CO.

In Figure 7, a 2.2% Rh/ $\text{Al}_2\text{O}_3$  sample was first saturated at 310K with CO, giving the infrared spectrum shown in 6(a), which is typical for pure CO adsorption (14, 15, 18, 21). The CO was pumped away and the CO-saturated sample was exposed to  $\text{D}_2(\text{g})$  at 102 torr and 310K. Following 19 hours exposure spectrum 6(b) was obtained. There is some loss of intensity at  $2101\text{cm}^{-1}$  and at  $2031\text{cm}^{-1}$  corresponding to a decrease in the concentration of  $\text{Rh}(\text{CO})_2$  species. Similar effects have been observed during reversible thermal desorption of CO from these surfaces (14). In addition, slight exchange of  $\text{Al}_2\text{O}_3$ -bound hydrogen (AlOH) with deuterium

is observed by the appearance of enhanced intensity in a broad band with its peak maximum at  $2650\text{cm}^{-1}$ . This deuterium exchange at 310K occurs only with the involvement of Rh sites for chemisorptive  $\text{D}_2$  dissociation followed by D migration on the  $\text{Al}_2\text{O}_3$  and has been studied previously (23). An additional exposure to  $\text{D}_2(\text{g})$  at 282 torr resulted in only slight changes in intensity but yielded no additional infrared features. The cell was then evacuated,  $\text{CO}(\text{g})$  was added to resaturate the Rh surface, and the CO was then evacuated while cooling to 90K. The cell was then filled with 0.1 Torr of  $\text{D}_2(\text{g})$  and the tungsten atomization filament was turned on to bombard the surface with atomic D. A substantial drop in  $\text{D}_2(\text{g})$  pressure occurred, and the substrate temperature increased to 170K. Infrared spectra corresponding to various amounts of atomic D bombardment of the surface are shown in Figure 7(c) and 7(d). A total exposure to  $\sim 2 \times 10^{19}$  D atoms corresponds to spectrum 7(d). No new spectral features were observed during this treatment.

## V. DISCUSSION

### A. The Infrared Spectrum of the HCO Ligand

Using matrix isolation techniques, the infrared spectrum of HCO has been measured in a CO matrix at 14-20K (24,25). It exhibits a  $\text{C}=\text{O}$  stretching mode at  $1860\text{cm}^{-1}$ , an intense  $\text{C}-\text{H}$  stretching mode at  $2488\text{cm}^{-1}$  (25), and a  $\text{H}-\text{C}=\text{O}$  bending vibration at  $1090\text{cm}^{-1}$  (24,25). HCO is characterized by a weak  $\text{C}-\text{H}$  bond and by a corresponding high  $\text{C}=\text{O}$  stretching frequency (25,26). Synthesis of matrix isolated HCO is

achieved at low temperatures by the interaction of energetic (photolytically produced) H atoms with a CO matrix. In attempts to use thermalized H atoms reacting with CO in an Ar matrix, no reaction has been observed (27).

When HCO is bound as a ligand to transition metal atoms, the C=O stretching frequency is usually observed to shift downwards to  $1600\text{cm}^{-1}$  and an increase of  $100\text{-}200\text{cm}^{-1}$  in the CH stretching frequency is observed. A summary of information regarding characteristic frequencies for the HCO moiety is given in Table II.

Based on Table II it would seem appropriate to search for HCO (ads) infrared features in the range  $1500\text{-}1800\text{cm}^{-1}$  ( $\nu_{\text{C-O}}$ ) and in the range  $2500\text{-}2700\text{cm}^{-1}$  ( $\nu_{\text{H-C}}$ ). The bending vibration below  $1100\text{cm}^{-1}$  is in an experimentally difficult region in this work due to strong absorption by the  $\text{Al}_2\text{O}_3$  support.

B. Lack of Evidence for Production of HCO (ads) from either  $\text{H}_2\text{CO}$  or  $(\text{HCO})_2$  on  $\text{Rh}/\text{Al}_2\text{O}_3$ .

By comparison of the infrared spectra (Fig. 2 and 3) for  $\text{H}_2\text{CO}$  on  $\text{Al}_2\text{O}_3$  and on  $\text{Rh}/\text{Al}_2\text{O}_3$ , it is evident that under no condition of temperature utilized here is there evidence for additional absorption bands on the  $\text{Rh}/\text{Al}_2\text{O}_3$  surface in either the  $1500\text{-}1800\text{cm}^{-1}$  region or the  $2500\text{-}2700\text{cm}^{-1}$  region. On this basis we can be confident that HCO (ads) is not produced at a spectroscopically detectable level on Rh from  $\text{H}_2\text{CO}$  adsorbate.

The same comparison may be made for  $(\text{HCO})_2$  adsorbate. Here too, no extra absorption bands related to  $\text{HCO (ads)}$  species on Rh are detected in the  $1500\text{--}1800\text{cm}^{-1}$  region or the  $2500\text{--}2700\text{cm}^{-1}$  region. Thus  $(\text{HCO})_2$  is also not a favorable source of  $\text{HCO (ads)}$  on an  $\text{Al}_2\text{O}_3$ -supported Rh surface.

C. Atomic Deuterium + CO (ads). Lack of Evidence for DCO (ads) by this Route.

Although expected to be an unlikely route to  $\text{DCO (ads)}$  formation, a chemisorbed CO layer on Rh was exposed to thermalized D atoms at  $\sim 170\text{K}$ . The D-CO stretching frequency would be expected at about  $2000\text{cm}^{-1}$  for  $\text{DCO (ads)}$ . The  $\text{DC}\equiv\text{O}$  stretching frequency would be expected between  $1800\text{cm}^{-1}$  and about  $1550\text{cm}^{-1}$  (25) [See also Table II]. Although the  $2000\text{cm}^{-1}$  region is strongly overlapped by chemisorbed CO intensity, there is no evidence in either region for additional absorption due to the formation of  $\text{DCO (ads)}$  species.

D. Interaction of  $\text{H}_2\text{CO}$  and  $(\text{HCO})_2$  with Rh/ $\text{Al}_2\text{O}_3$ .

The similarity in the infrared spectra for species produced on Rh from  $\text{H}_2\text{CO}$  and from  $(\text{HCO})_2$  is evident by comparison of Figures 3 and 6. On the basis of comparisons with intensities achieved for pure CO adsorption, it is clear that both  $\text{H}_2\text{CO}$  and  $(\text{HCO})_2$  yield appreciable quantities of both terminal-CO and bridged-CO species. These species are present on the crystalline Rh sites described previously (14,18). The  $\text{Rh(CO)}_2$  species are not strongly populated by exposure to  $\text{H}_2\text{CO}$  or  $(\text{HCO})_2$ , but

may be filled by subsequent CO adsorption. A previous model suggested to explain this lack of production of  $\text{Rh}(\text{CO})_2$  from  $\text{H}_2\text{CO}$  adsorption postulated the formation of H-Rh-CO species from  $\text{H}_2\text{CO}$  (21). This picture was based on the observation of a shifted  $\text{Rh}(\text{CO})_2$  doublet when  $\text{H}_2\text{CO} + \text{CO}$  were adsorbed. The work reported here in section III.C. has shown that this shift was in fact due to interaction of the  $\text{Rh}(\text{CO})_2$  with adsorbates produced by  $\text{H}_2\text{CO}$  on the  $\text{Al}_2\text{O}_3$  support. We now believe that neither  $\text{H}_2\text{CO}$  nor  $(\text{HCO})_2$  decompose appreciably on the isolated Rh sites.

Two factors may be responsible for this low reactivity of the isolated Rh sites:

- (1) both  $\text{H}_2\text{CO}$  and  $(\text{HCO})_2$  require multiple sites to dissociatively chemisorb
- (2) the special electronic character of isolated Rh sites prohibits dissociative chemisorption of  $\text{H}_2\text{CO}$  and  $(\text{HCO})_2$ . There is evidence that the isolated sites are in fact  $\text{Rh}^+$  species (18). Primet and Garbowski have assigned these sites as Rh(I) based on UV-visible absorption spectral studies of a Rh-Na zeolite (30).

#### E. Interaction of $\text{H}_2\text{CO}$ with $\text{Al}_2\text{O}_3$ .

Upon warming the  $\text{H}_2\text{CO}/\text{Al}_2\text{O}_3$  sample from 100K to 300K, several distinct transitions occur. By 160K, the intensity of the  $3730$  and  $3660\text{cm}^{-1}$  features due to free OH on  $\text{Al}_2\text{O}_3$  was decreased by a factor of two, while the broad hydrogen bonded OH feature near  $3500\text{cm}^{-1}$  has increased in intensity significantly. Previous work on silica surfaces (31,32) has shown that free OH features can be shifted by as much as  $350\text{cm}^{-1}$  to lower wavenumber due to interaction with  $\text{R}_2\text{CO}$  groups. We

therefore suggest that at 160K, evidence for a site specific interaction of  $\text{H}_2\text{CO}$  on  $\text{Al}_2\text{O}_3$  exists.

Simultaneously, distinct features appear at lower wavenumber which indicate the presence of molecularly adsorbed  $\text{H}_2\text{CO}$  (see Table III). The observed shifts and/or multiple peaks observed for  $\nu_5$ ,  $\nu_4$ ,  $\nu_3$  and  $\nu_2$  could be attributed to either;

- a) a single binding site on  $\text{Al}_2\text{O}_3$  which reduces the symmetry of the adsorbed species from the gas phase symmetry of  $\text{C}_{2v}$ .
- b) adsorption at a number of distinct binding sites.

Additional warming serves to clarify the situation. Once the sample has reached room temperature, all of the features observed at 200K (with the exception of the  $1470\text{cm}^{-1}$  feature) have maximized in strength, and have begun to diminish. Three new features have also become apparent, dominating figure 2e at  $1392$ ,  $1372$  and  $1594\text{cm}^{-1}$ . Greenler (17) has attributed these modes to formate ( $\text{HCOO}$ ) formation from  $\text{CH}_3\text{OH}$  decomposition on  $\text{Al}_2\text{O}_3$ . Evacuation of the sample further reduces the intensity above  $1700\text{cm}^{-1}$  and below  $1350\text{cm}^{-1}$ . In most of the spectral regions of interest, it is not possible to make a meaningful measure of the loss of intensity, since formate modes and formaldehyde modes will be unresolved. For instance, in the C-H stretching region, as the conversion of  $\text{H}_2\text{CO}$  to formate occurs, the contributions from the formate C-H stretch (17b) would be expected to compensate for loss of formaldehyde C-H stretch absorption. However, the  $\text{CH}_2$  deformation mode observed at  $1470\text{cm}^{-1}$  is spectrally isolated from any formate modes. This feature neither shifts nor changes in intensity after the sample has reached 200K. This clearly indicates the presence of a site which

is stable for formaldehyde bonding between 200 and 310K. Thus, at least two sites exist for the binding of  $\text{H}_2\text{CO}$  to  $\text{Al}_2\text{O}_3$ . One site associated with the  $\text{CH}_2$  mode at  $1470\text{cm}^{-1}$ , and another site on which formaldehyde converts to formate.

#### F. Interaction of $(\text{HCO})_2$ with $\text{Al}_2\text{O}_3$ .

In the process of carrying out the control experiments with  $(\text{HCO})_2$  on  $\text{Al}_2\text{O}_3$ , an interesting temperature dependence was observed in the infrared spectra, as shown in Figure 5. At temperatures below about  $\sim 250\text{K}$ , the dominant carbonyl stretching feature is seen at  $1720\text{cm}^{-1}$ ; upon warming above  $250\text{K}$ , the  $1720\text{cm}^{-1}$  feature disappears and a  $1748\text{cm}^{-1}$  feature is enhanced. The species corresponding to the  $1748\text{cm}^{-1}$  feature is involatile at  $305\text{K}$  as shown in spectrum 5(e).

We assign the  $1720\text{cm}^{-1}$  feature to monomeric  $(\text{HCO})_2$  adsorbed on  $\text{Al}_2\text{O}_3$ . For comparison  $(\text{HCO})_2(\text{g})$  exhibits a fundamental  $\nu_{\text{CO}}$  of  $1745\text{cm}^{-1}$  (35).  $(\text{HCO})_2$  may exist as a cis or trans isomer, but both isomers have been shown to exhibit a  $\nu_{\text{CO}}$  within  $1\text{cm}^{-1}$  of each other. Thus, the adsorption by  $\text{Al}_2\text{O}_3$  of  $(\text{HCO})_2$  monomer is associated with a  $25\text{cm}^{-1}$  decrease in  $\nu_{\text{CO}}$ , compared to  $(\text{HCO})_2(\text{g})$ . In this context, we have observed that physisorbed  $^{13}\text{CO}$  on  $\text{Al}_2\text{O}_3$  at  $100\text{K}$  produces an absorption band at  $2190\text{cm}^{-1}$ , or a shift to higher wavenumber of  $13\text{cm}^{-1}$  from the gas value. This suggests that the monomer  $(\text{HCO})_2$  (ads) is rather strongly perturbed electronically in its adsorptive interaction with  $\text{Al}_2\text{O}_3$ .

The  $1748\text{cm}^{-1}$  feature which forms extensively above  $\sim 250\text{K}$  is assigned as a polymer of  $(\text{HCO})_2$ . It is well known that  $(\text{HCO})_2$  will polymerize

easily and Harris (34) has published an infrared spectrum of the polymer which coated his gas cell windows during IR studies of  $(\text{HCO})_2(\text{g})$ . Careful measurement of the literature spectrum indicate that  $\nu_{\text{CO}}$  for this polymer was observed at  $1747\text{cm}^{-1}$ , in good agreement with our feature on  $\text{Al}_2\text{O}_3$  at  $1748\text{cm}^{-1}$ .

Features in the C-H stretching region at  $2930\text{cm}^{-1}$  and  $2840\text{cm}^{-1}$  are assigned as polymer and monomer species respectively and their relative intensity changes on warming roughly parallel the  $\nu_{\text{CO}}$  intensity changes.  $(\text{HCO})_2(\text{g})$  exhibits  $\nu_{\text{CH}}=2844\text{cm}^{-1}$  (34), in good agreement with this assignment, whereas the condensed polymer exhibits a weak C-H stretching mode at  $2924\text{cm}^{-1}$  (34).

#### VII. SUMMARY

- (1) The adsorption of  $\text{H}_2\text{CO}$  or  $(\text{HCO})_2$  on  $\text{Rh}/\text{Al}_2\text{O}_3$  surfaces produces species having similar infrared spectra in the carbonyl-stretching region. These species resemble chemisorbed CO at low coverages on crystalline Rh sites. However the  $\text{Rh}(\text{CO})_2$  species observed for CO adsorption on isolated  $\text{Rh}^+$  sites are not readily produced from either  $\text{H}_2\text{CO}$  or  $(\text{HCO})_2$ .
- (2) No spectral evidence is found for the stabilization of chemisorbed HCO (or DCO) species on  $\text{Al}_2\text{O}_3$ -supported Rh when  $\text{H}_2\text{CO}$ ,  $(\text{HCO})_2$ , or atomic D+CO(ads) are used as potential sources of chemisorbed HCO (or DCO).
- (3) Stable surface species are produced from the interaction of  $\text{H}_2\text{CO}$  or  $(\text{HCO})_2$  with  $\text{Al}_2\text{O}_3$ .

We conclude that quantities of HCO(ads) species cannot be stabilized by chemisorption on Rh surfaces or on  $\text{Rh}^+$  sites present on  $\text{Al}_2\text{O}_3$ -supported

Rh, even at low temperatures. This observation suggests that mechanisms involving adsorbed hydrogen atom attack on chemisorbed CO to eventually produce hydrocarbon products may be unrealistic.

\*\* The identification of specific suppliers and manufacturers is provided to aid the reader. No endorsement of this product by NBS is implied.

#### VIII. ACKNOWLEDGEMENTS

The authors would like to thank Dr. S. M. Girvin and Dr. T. M. Duncan for many profitable discussions. This work is partially supported by the Office of Naval Research, Contract *N00014-81-F-0008*

## REFERENCES

1. (a) D. W. Goodman, R. D. Kelley, T. E. Madey, and J. T. Yates, Jr., *J. Catal.* **63**, 226-234 (1980).  
(also see earlier references therein to work on supported Ni which originally suggested a dissociative CO mechanism).  
(b) For a recent review, see V. Ponec, *Cat. Rev. Sci. Engr.*, **18**, 151 (1978).
2. John G. Ekerdt and A. T. Bell, *J. Catal.*, **58**, 170 (1979).
3. J. A. Rabo, A. P. Risch and J. L. Poutsma, *J. Catal.* **53**, 295 (1978).
4. R. A. Della Betta and M. Shelef, *J. Catal.*, **48**, 111 (1977); see also *J. Catal.*, **60**, 169 (1979).
5. B. A. Sexton and G. A. Somorjai, *J. Catal.*, **46**, 167 (1977).
6. D. G. Costner and G. A. Somorjai, *Surf. Sci.*, **83**, 60 (1979).
7. J. T. Yates, Jr., E. D. Williams, and W. H. Weinberg, *Surf. Sci.*, **91**, 562 (1980); see also D. G. Costner, L. H. Dubois, B. A. Sexton, and G. A. Somorjai, *Surf. Sci.*, 103 (1981) L134.
8. E. L. Muetterties and J. Stein, *Chem. Rev.*, **79**, 479 (1979).
9. G. A. Mills and F. W. Steffgen, *Catal. Rev.*, **8** (2), 159 (1973).
10. D. W. Goodman, T. E. Madey, M. Ono, and J. T. Yates, Jr., *J. Catal.*, **50**, 279 (1977).
11. J. T. Yates, Jr., T. E. Madey, and M. J. Dresser, *J. Catal.*, **30**, 260 (1973).
12. S. D. Worley and J. T. Yates, Jr., *J. Catal.*, **48**, 395 (1977).
13. (a) T. J. Collins and W. R. Roper, *JCS Chem. Comm.*, p. 1044, (1976).  
(b) R. L. Pruett, R. C. Schoening, J. L. Vidal, and R. A. Fiato, *J. Organometallic Chem.*, **182**, C57 (1979).  
(c) J. A. Gladysz and J. C. Seiver, *Tetrahedron Letters*, **4** 319 (1978).
14. J. T. Yates, Jr., T. M. Duncan, S. D. Worley, and R. W. Vaughan, *J. Chem. Phys.*, **70**, 1219 (1979).
15. R. R. Cavanagh and J. T. Yates, Jr., *J. Chem. Phys.*, accepted.
16. R. G. W. Norrish and G. A. Griffiths, *Journal of the Chemical Society*, 2829 (1928).

17. (a) R. G. Greenler, J. Chem. Phys. 37, 2094 (1962);  
(b) J. D. Donaldson, J. F. Knifton and S. D. Ross, Spectrochimica ACTA 20, 847 (1964);  
(c) Y. Noto, K. Fukuda, T. Onishi and K. Tamaru, Trans. Faraday Soc. 63, 2300 (1967);  
(d) M. Ito and W. Syetake, J. Phys. Chem. 79, 1190 (1975).
18. R. R. Cavanagh and J. T. Yates, Jr., J. Chem. Phys., (accepted).
19. P. A. Thiel, E. D. Williams, J. T. Yates, Jr., and W. H. Weinberg, Surface Sci., 84, 199 (1979).
20. L. H. Dubois and G. A. Somorjai, Surface Sci., 91, 514 (1980).
21. J. T. Yates, Jr. S. D. Worley, T. M. Duncan, and R. W. Vaughan, J. Chem. Phys., 70, 1225 (1979).
22. E. D. Williams, P. A. Thiel, W. H. Weinberg, and J. T. Yates, Jr. J. Chem. Phys., 72, 3496 (1980).
23. R. R. Cavanagh and J. T. Yates, Jr., J. Catalysis, (in press).
24. G. E. Ewing, W. E. Thompson and G. C. Pimentel, J. Chem. Phys., 32, 927 (1960).
25. D. E. Milligan and M. E. Jacox, J. Chem. Phys., 41, 3032 (1964).
26. F. J. Adrian, E. D. Cochran and V. A. Bowers, J. Chem. Phys., 36, 1661 (1962).
27. D. E. Milligan and M. E. Jacox, J. Chem. Phys., 38, 2627 (1963).
28. C. P. Casey and S. M. Neumann, J. Amer. Chem. Soc., 98, 5395 (1976).
29. J. P. Collman and S. R. Winter, J. Amer. Chem. Soc., 95, 4089 (1973).
30. M. Primet and E. Garbowski, Chem. Phys. Letters, 72, 472 (1980).
31. A. N. Sidorov, Zh. fiz. khim. 30, 995 (1956).
32. V. Ya. Davydov, A. V. Kiselev, and B. D. Kuznetsov., Zh. fiz. khim. 39, 2058 (1965).
33. G. Herzberg, Molecular Spectra and Molecular Structure II. Infrared and Raman Spectra of Polyatomic Molecules. Van Nostrand Reinhold. Co. New York, (1945).
34. R. K. Harris, Spectrochim Acta 20, 1129 (1964).

### FIGURE CAPTIONS

- Fig. 1 Variable temperature infrared cell. - The tungsten filament for dissociation of  $D_2$  to atomic D is indicated, as is the radiation shield.
- Fig. 2. Infrared spectrum of  $H_2CO$  adsorbed on  $Al_2O_3$ . The sample is dosed with formaldehyde while at 100K (a). Spectrum b-d indicate changes while warming to the indicated temperature. Spectrum (e) was recorded after evacuating the sample to  $\sim 1 \cdot 10^{-5}$  Torr.
- Fig. 3. Infrared spectrum of  $H_2CO$  chemisorbed on  $Rh/Al_2O_3$ . (a)-(c) correspond to the spectral developments following introduction of  $H_2CO$  at 80K. Subsequent evacuation and saturation with CO resulted in spectrum (d).
- Fig. 4. Perturbation of  $^{13}CO$  (ads) on  $Rh/Al_2O_3$  following exposure to  $H_2$   $^{12}CO(g)$ .
- Fig. 5. Infrared spectrum of glyoxal  $(HCO)_2$  adsorbed on  $Al_2O_3$ .
- Fig. 6. Infrared spectrum of  $(HCO)_2$  chemisorbed on  $Rh/Al_2O_3$ .
- Fig. 7. Interaction of atomic deuterium with chemisorbed CO on  $Rh/Al_2O_3$ .

TABLE I  
INFRARED FEATURES OBSERVED FOR  $\text{H}_2\text{CO}$   
ADSORPTION ON  $\text{Al}_2\text{O}_3$   
( $\text{cm}^{-1}$ )

Sample Temperature (K)	<200	200-300	>300 +evacuation
	2977	2977	2962
	2913	2913	2908
	2788	2788	2788
	2040 (br)		
	1700	1770-1700	1770-1700
		1594	1594
		1392	1392
		1372	1372
	1470	1470	1470
	1430	1430	unresolved
	1395	1395	
	1280	1280	1300
	1230	1230	1230
	1150	1150	1150

TABLE II  
INFRARED FREQUENCIES OBSERVED FOR  
THE HCO LIGAND

MOLECULE	Wavenumber (cm <sup>-1</sup> )			REF
	$\nu_{C-H}$	$\nu_{C=O}$	$\nu_{HCO}$ (bend)	
HCO (in CO matrix)	2488	1861	1090	25
Os(HCO) Cl(CO) <sub>2</sub> (PPh <sub>3</sub> ) <sub>2</sub>		1610		13(a)
[Ir <sub>4</sub> (CO) <sub>11</sub> (HCO)] <sup>-</sup>		1590-1610		13(b)
$\left[ \begin{array}{c} \text{(CO)}_4 \text{ Mn} \begin{array}{l} \text{H} \diagup \text{C=O} \\ \text{C=O} \diagdown \text{Ph} \end{array} \end{array} \right]^-$		1588		13(c)
$\left[ \begin{array}{c} \text{(CO)}_4 \text{ Mn} \begin{array}{l} \text{H} \diagup \text{C=O} \\ \text{C=O} \diagdown \text{CH}_3\text{OCH}_2 \end{array} \end{array} \right]^-$		1604		13(c)
$\left[ \begin{array}{c} \text{C}_5\text{H}_5(\text{CO}) \text{ Fe} \begin{array}{l} \text{H} \diagup \text{C=O} \\ \text{C=O} \diagdown \text{Ph} \end{array} \end{array} \right]^-$		1555		13(c)
[Et <sub>4</sub> N] [(PhO) <sub>3</sub> P] (CO) <sub>3</sub> FeHCO		1584		28
[(CO) <sub>4</sub> Fe (CHO)] <sup>-</sup>	2690 2540	1577-1610		29

# Variable Temperature Infrared Cell

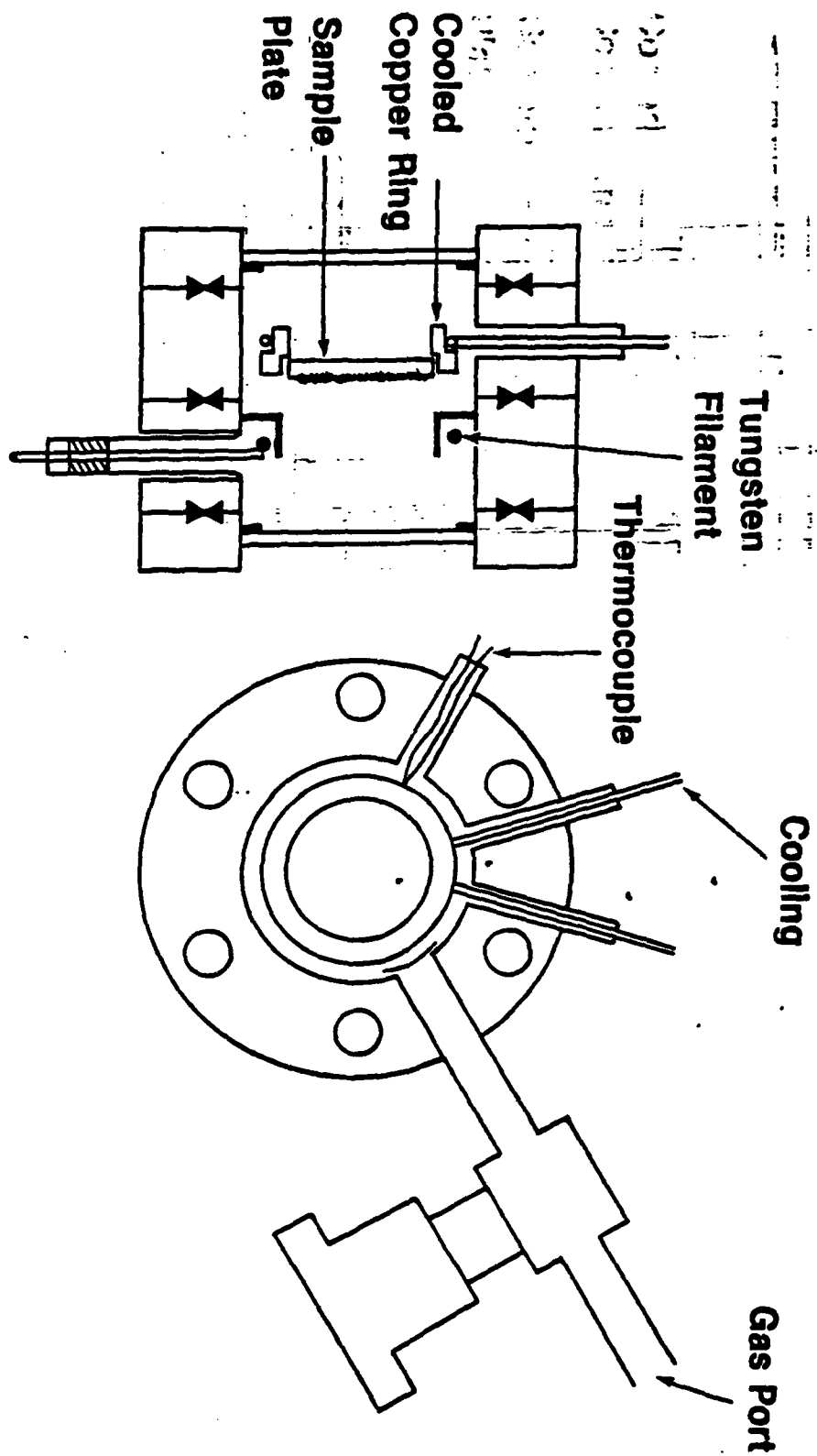


Figure 1

# Infrared Spectrum of $\text{H}_2\text{CO}$ Adsorbed on $\text{Al}_2\text{O}_3$

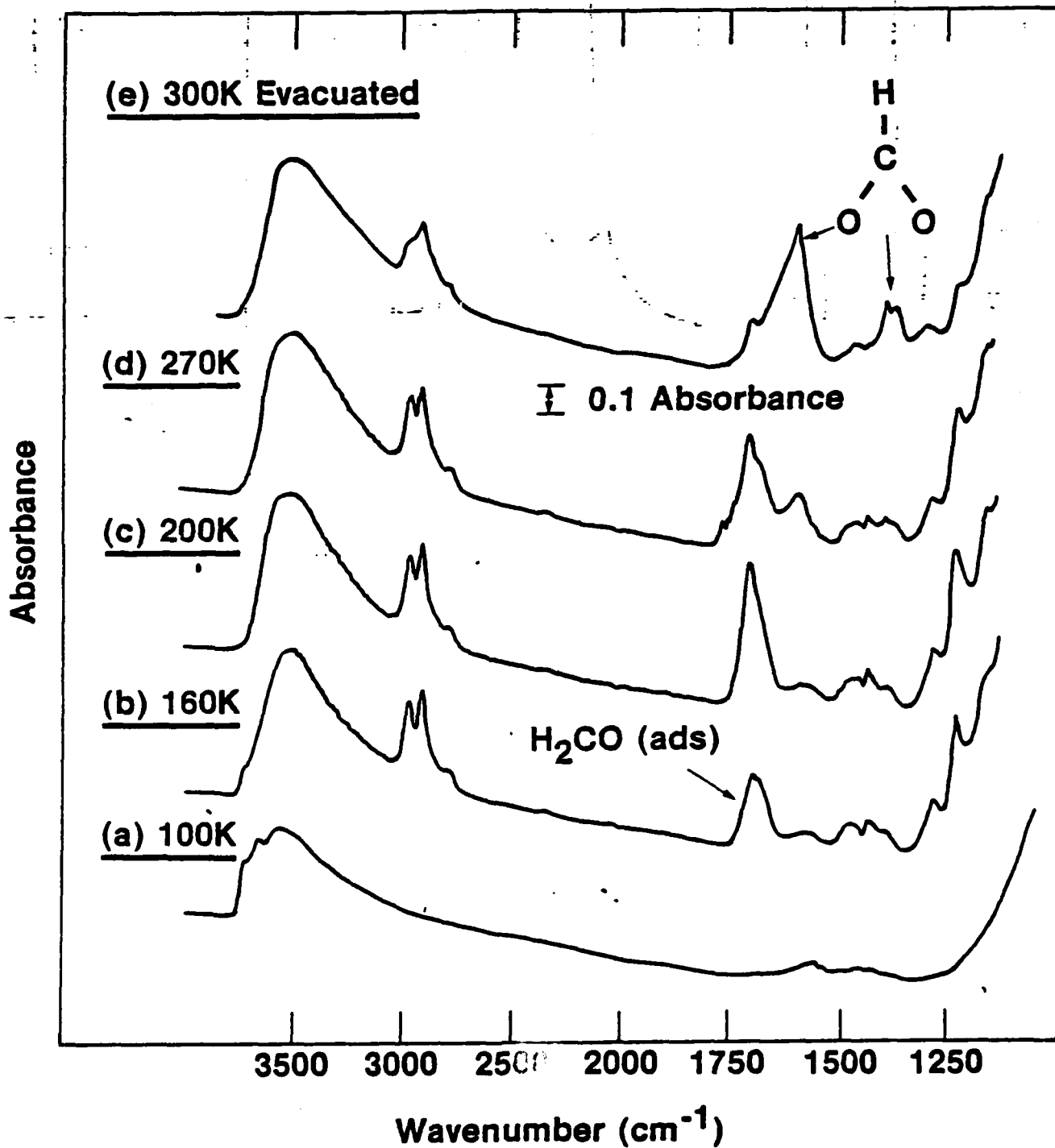


Figure 2

Infrared Spectrum of  $\text{H}_2\text{CO}$   
Chemisorbed on  $\text{Rh}/\text{Al}_2\text{O}_3$

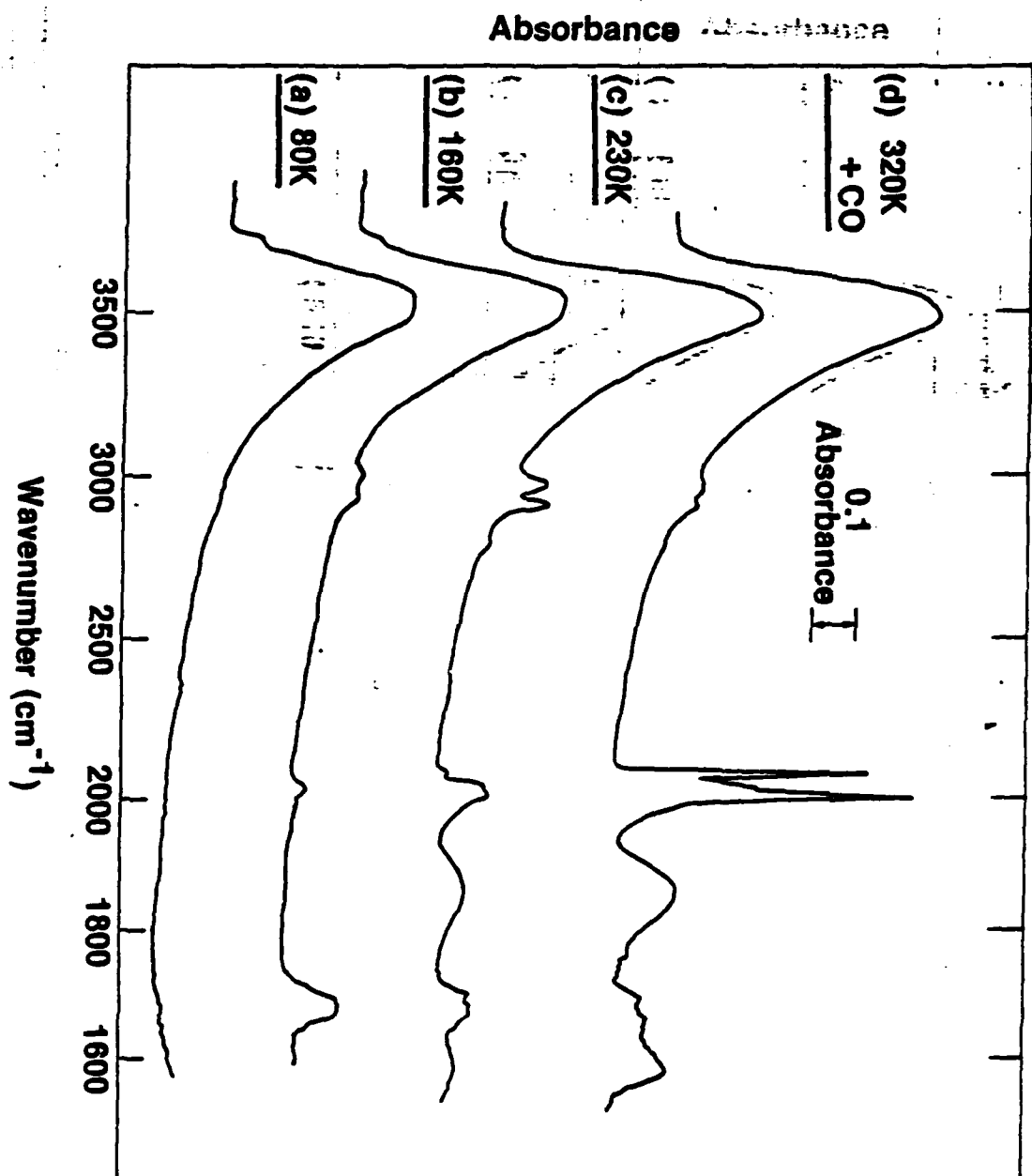


Figure 3

Perturbation of  $^{13}\text{CO}$  (ads) on  $\text{Rh}/\text{Al}_2\text{O}_3$   
Following Exposure to  $\text{H}_2^{12}\text{CO}$  (g)

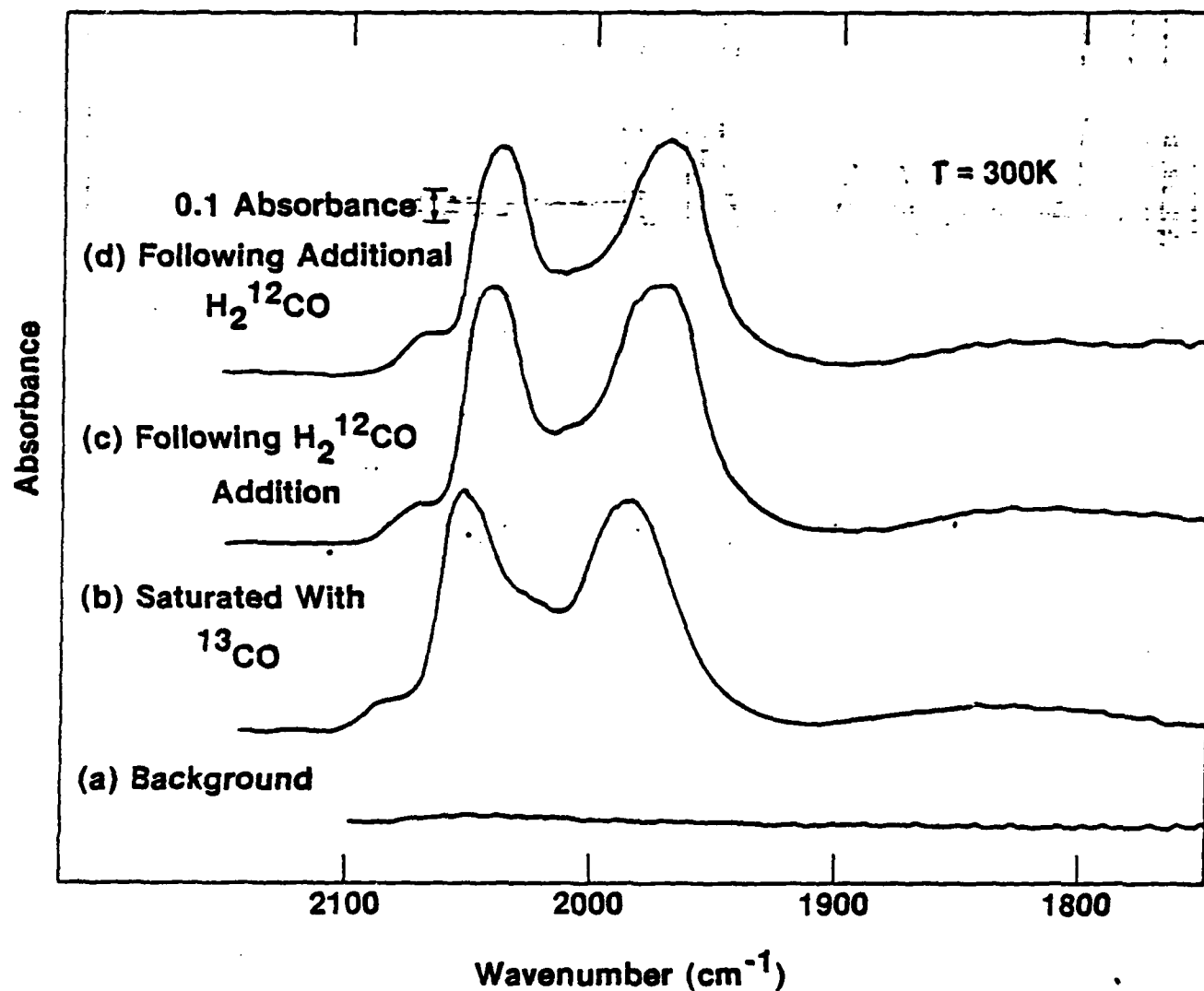


Figure 4

Infrared Spectrum of  $(\text{HCO})_2$   
Adsorbed on  $\text{Al}_2\text{O}_3$

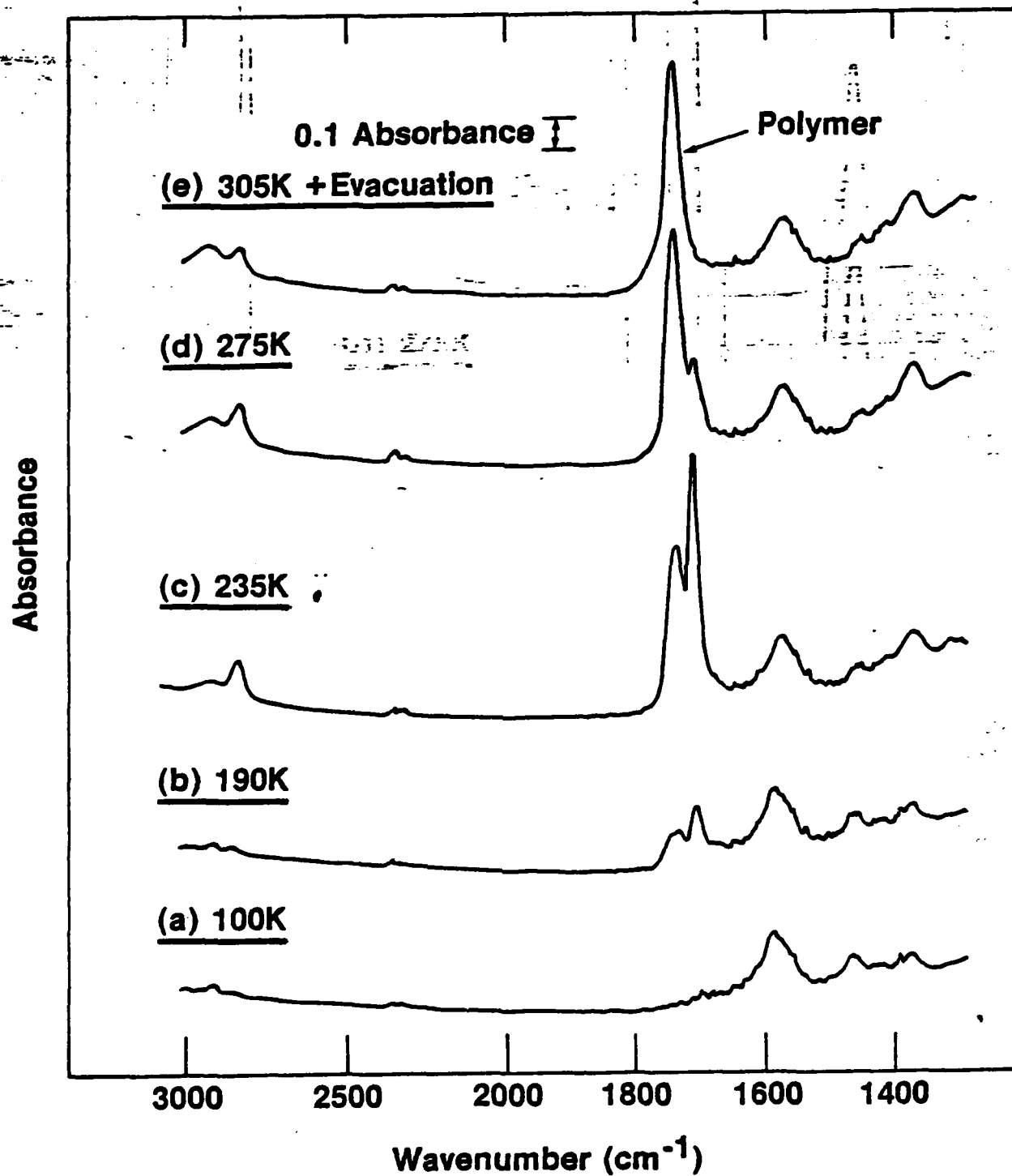


Figure 5

Infrared Spectrum of  $(\text{HCO})_2$   
Chemisorbed on  $\text{Rh}/\text{Al}_2\text{O}_3$

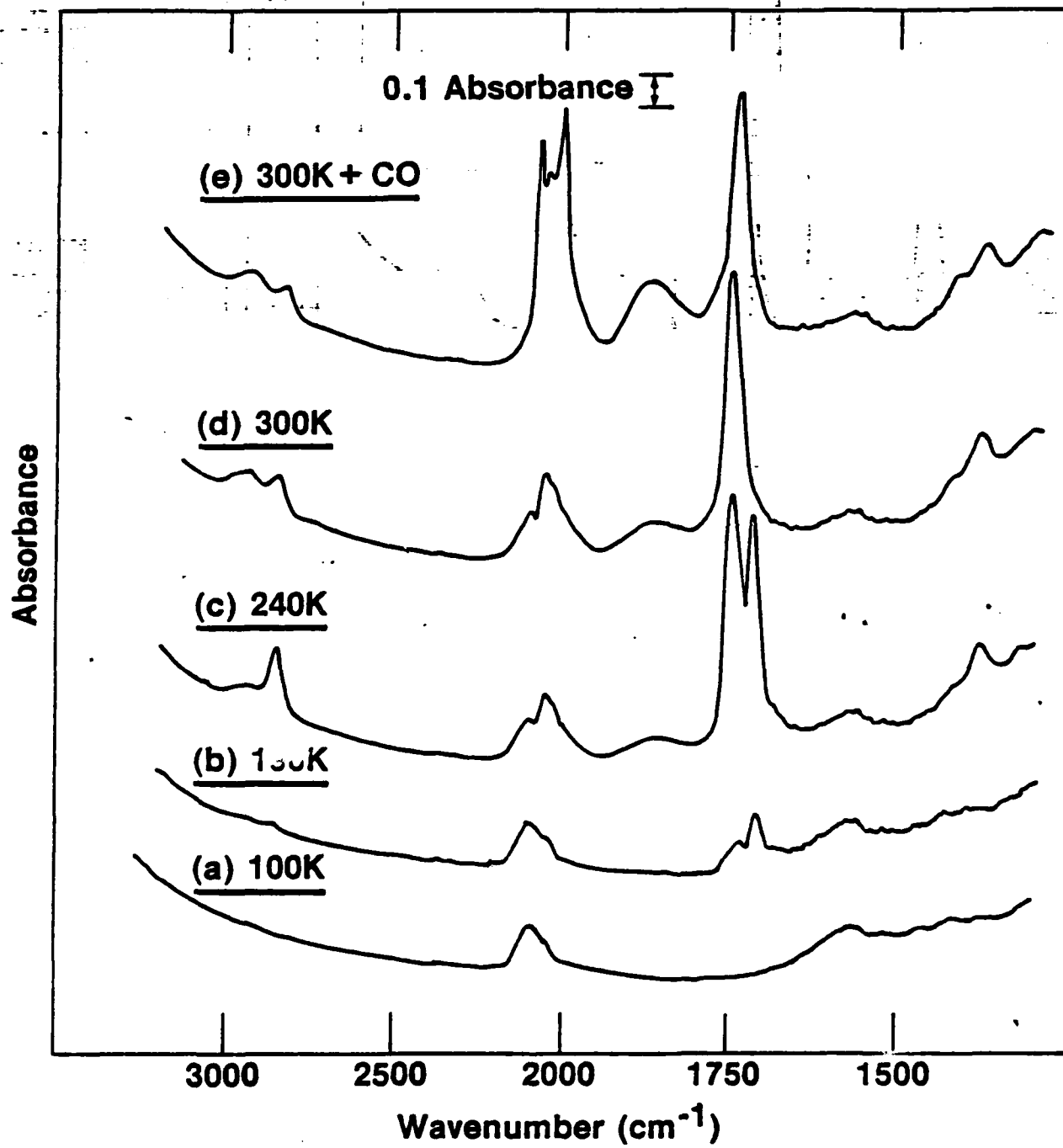


Figure 6

# Interaction of Atomic Deuterium With Chemisorbed CO on Rh/Al<sub>2</sub>O<sub>3</sub>

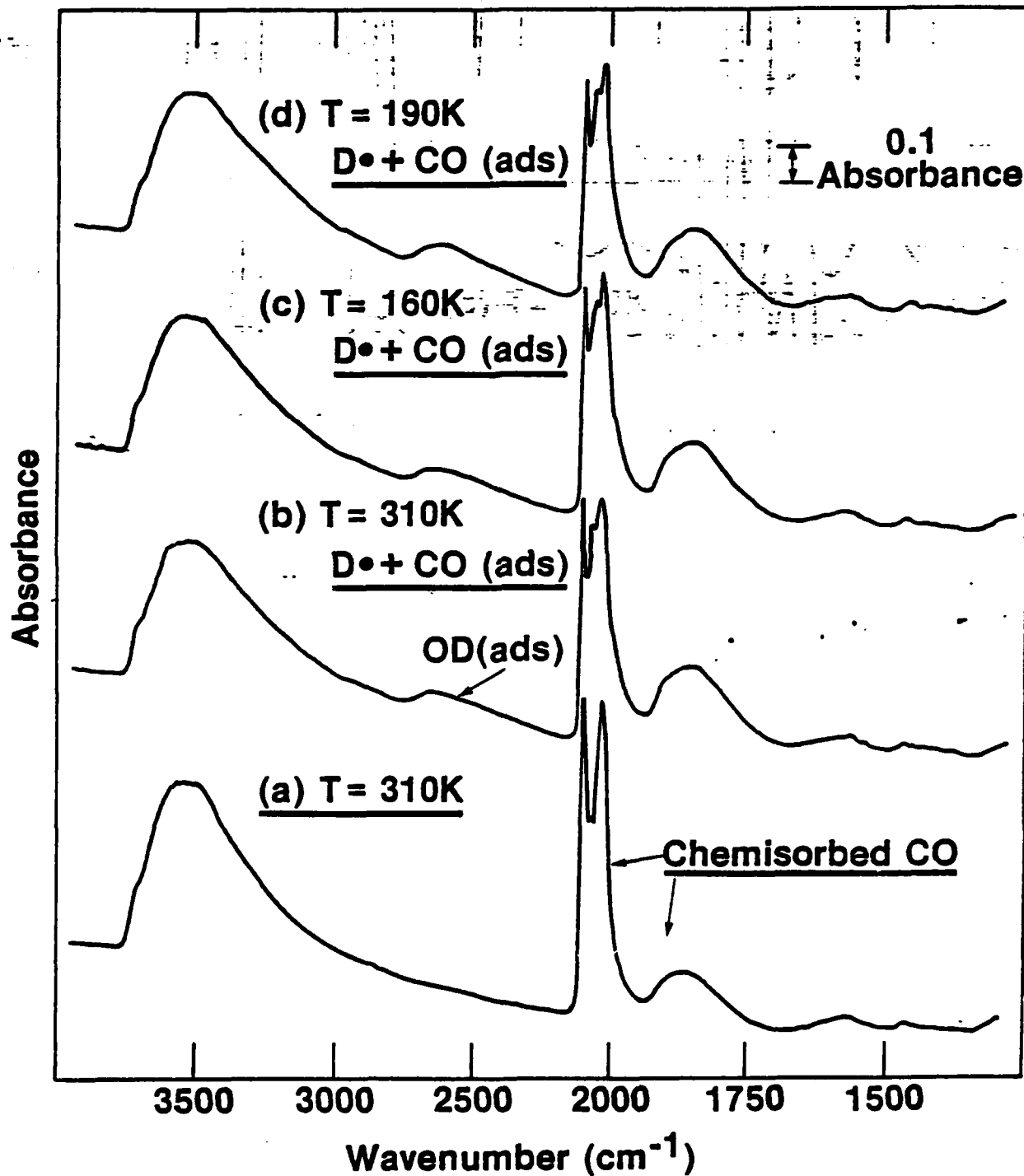


Figure 7